TIGHT JUNCTIONS IN THE CHOROID PLEXUS EPITHELIUM

A Freeze-Fracture Study Including Complementary Replicas

B. VAN DEURS and J. K. KOEHLER

From the Department of Biological Structure, University of Washington School of Medicine, Seattle, Washington 98195. Dr. van Deurs' present address is Anatomy Department A, University of Copenhagen, 2200 Copenhagen N., Denmark.

ABSTRACT

The tight junctions of the choroid plexus epithelium of rats were studied by freeze-fracture. In glutaraldehyde-fixed material, the junctions exhibited rows of aligned particles and short bars on P-faces, the E-faces showing grooves bearing relatively many particles. A particulate nature of the junctional strands could be established by using unfixed material. The mean values of junctional strands from the lateral, third, and fourth ventricles of Lewis rats were 7.5 ± 2.6, 7.4 ± 2.2, and 7.5 ± 2.4; and of Sprague-Dawley rats 7.7 ± 3.4, 7.4 ± 2.3, and 7.3 ± 1.6. Examination of complementary replicas (of fixed tissue) showed that discontinuities are present in the junctional strands: 42.2 ± 4.6% of the length of measured P-face ridges were discontinuities, and the total amount of complementary particles in E-face grooves constituted 17.8 ± 4.4% of the total length of the grooves, thus ~25% of the junctional strands can be considered to be discontinuous. The average width of the discontinuities, when corrected for complementary particles in E-face grooves, was 7.7 ± 4.5 nm. In control experiments with a "tighter" tight junction (small intestine), complementary replicas revealed that the junctional fibrils are rather continuous and that the very few particles in E-face grooves mostly filled out discontinuities in the P-face ridges. ~5% of the strands were found to be discontinuous. These data support the notion that the presence of pores in the junctional strands of the choroid plexus epithelium may explain the high transepithelial conductance in a "leaky" epithelium having a high number of junctional strands. However, loss of junctional material during fracturing is also considered as an alternative explanation of the present results.

KEY WORDS freeze fracture · complementary replicas · choroid plexus epithelium · tight junctions · permeability properties

The choroid plexus functions in the secretion of the cerebrospinal fluid (CSF) (8). The epithelium is provided with a ouabain-sensitive Na^+-K^+-ATPase at the apical surface and actively pumps ions from the blood side of the epithelium into the CSF (21, 33, 34). In addition, a major pathway for passive ion permeation is believed to exist via the intercellular spaces and cell junctions (33, 34). This view is based upon electrophysiological observations which show that the choroid plexus epithelium exhibits a low transepithelial resistance (32–34) and thus is classified as a "leaky" epithe-

J. CELL BIOLOGY © The Rockefeller University Press · 0021-9525/79/03/0662-12$1.00
Volume 80 March 1979 662–673

lium (7). Claude and Goodenough (7) correlated the "tightness" of tight junctions with the number of strands, and according to their data the choroid plexus should exhibit relatively few junctional strands (<5). Claude and Goodenough (7) also found that in leaky epithelia there apparently were discontinuities in the strands but assumed that complementary particles present in the E-face grooves accounted for these discontinuities. Similarly, Brightman et al. (1, 2) described discontinuities in the tight junctional strands of the choroid plexus, but these authors proposed that such discontinuities underlie the "leaky" permeability characteristics of the plexus epithelium. One approach to actually documenting the presence of discontinuities or "pores" in junctional strands would be the examination of complementary replicas (3, 5, 6, 17, 18, 31).

The present study further investigates structural aspects of the choroid plexus epithelial junctions particularly with respect to the number of junctional strands and to the existence of "pores" in these strands. It is demonstrated by freeze-fracture that the tight junctions of the plexus epithelium exhibit a higher number of junctional strands than expected from electrophysiological data (7, 32–34). Complementary replicas, however, show that the junctional strands are not continuous fibrils as seen in "tighter" tight junctions but exhibit discontinuities which may represent hydrated channels, thus explaining the leakiness of the choroid plexus epithelium. Portions of this study have been presented in preliminary form (26, 27).

MATERIALS AND METHODS

9 Lewis rats and 8 Sprague-Dawley rats (males, 2- to 3-mo-old) were used. The rats were anesthetized with ether, and the brains were rapidly removed and in most cases cut transversely into 5–7 slices before fixation by immersion in 2.5% glutaraldehyde in 0.1 M cacodylate buffer, pH 7.2° at 4°C. After 2–4 h of fixation, the choroid plexuses from the lateral, third, and fourth ventricles were removed and rinsed in 0.1 M cacodylate buffer. Specimens were kept for ~1 h in 15% glycerol in 0.1 M cacodylate buffer, and thereafter for at least 1 h in 30% glycerol in 0.1 M cacodylate buffer. Pieces of small intestine were fixed and cryoprotected in the same way. Furthermore, some pieces of small intestine were fixed for 60 min in 0.1% glutaraldehyde before cryoprotection (van Deurs and Luft, manuscript in preparation).

Routine Freeze-Fracture

Pieces of choroid plexuses and small intestine were frozen in liquid nitrogen-cooled Freon 22 and fractured in a Balzers BA-301 apparatus (Balzers Corp., Nashua, N. H.). Specimen stage temperature was −104°C, and the knife was cooled to at least −150°C before fracturing (recorded by an Omega digital temperature monitor connected to the microtome knife). The vacuum was always better than 2×10^{-5} Torr. Immediately after fracturing (etching was avoided), the specimens were shadowed with platinum-carbon. The uniformity of the shadowing thickness was checked with a Balzers quartz-crystal thin film monitor.

Direct Freezing of Tissue

Parts of the choroid plexuses (and small intestine) from several rats were rapidly removed, placed on gold disks (Balzers 4-position) and frozen directly (at ~−210°C) in a mixture of liquid and solid nitrogen prepared in a special vacuum Dewar similar to that described by MacKenzie (13). Freezing of metal-encased tissue in this apparatus is ~3 times faster than freezing in boiling nitrogen (13). Thereafter, the preparations were fractured as described under Routine Freeze Fracture. All fracture faces in this experimental group, as well as in the other groups, were determined by the curvature of the microvilli.

Preparation of Complementary (Double) Replicas

In these experiments, the Balzers double replica device was used. Two "double replica" specimen disks with central holes were apposed and filled with unfixed, noncryoprotected, or glutaraldehyde-fixed, glycerol-treated tissue and frozen in liquid-solid nitrogen as described above. This freezing technique was used since the tissue is almost completely encased by metal, and the freezing in liquid nitrogen-cooled Freon 22 therefore is rather slow, sometimes causing distinct ice crystal formation. Furthermore, freezing the double replica specimen disks in Freon results in solid Freon adhering to their surfaces after contact with liquid nitrogen, making it difficult or impossible to place the disks into the slits of the Balzers double replica device. The frozen specimen disks were inserted into the liquid nitrogen-cooled double replica device and transferred to the stage of the Balzers apparatus at −104°C. To avoid contamination of the fracture faces, the knife was cooled to at least −150°C, and platinum evaporation was begun immediately before fracturing. The rest of the procedure was as described for routine freeze-fracture. A total of nine pairs of good-quality complementary replicas of the choroid plexus, and six of the small intestine were examined and used for quantitation. Corresponding areas were obtained by photographing all junctions on both replicas, and then matching the negatives. The prints are mounted in a mirror image fashion, but the plane of the "mirror" is, for practical reasons, not necessarily the original plane. Therefore, the direction

of platinum shadowing on a double replica pair may not be the same.

Quantitation

The replicas were examined in a Philips 300 EM electron microscope calibrated with a carbon grating (54,864 lines/in.). The mean number of junctional strands (Table I, both P-face "ridges" and E-face "grooves" were included) was obtained by counting the number of strands along lines in the apical-basal direction which were 0.5 μm apart, at a magnification of 50,000 (7). The Student's t-test was used to evaluate statistical differences between the experimental data.

To measure the fraction (%) of junctional strands represented as discontinuities in P-face ridges and as transferred material (particles) on E-face grooves, complementary regions with tight junctions were used. Drawings of the junctional strands were made at a magnification of 140,000. The total length of junctional strands, and the total length of discontinuities were measured with a Hamilton map measurer. The fraction of particles in the complementary E-face grooves was calculated by counting particles in the grooves and multiplying the number by the average diameter of the particles (9.5 nm; value obtained by measuring the diameter of 100 particles from five different micrographs × 140,000 with a × 7 magnifying glass). Finally, the fraction of discontinuities in the junctional strands were calculated as the fraction of P-face discontinuities minus the fraction of E-face particles (Table II).

The width of the discontinuities in the P-face ridges was measured on prints (× 140,000) of complementary replicas with × 7 magnifying glass with a 0.1-mm scale, and then correcting for the presence of complementary particles in E-face grooves (Fig. 10).

RESULTS

General

The tight junction of the glutaraldehyde-fixed choroid plexus epithelium appears on P-fracture faces as a system of "ridges" formed by aligned particles (~10 nm in diameter) and short bars (~10 nm wide, and up to ~0.2 μm long in a few cases), with intervening "spaces" of various widths (Fig. 1). On E-faces the junction appears as a system of distinct, mostly continuous "grooves" (only a very few discontinuities were observed) containing scattered particles (~10 nm in diameter) (Fig. 2). Both the P-face ridges and the E-face grooves will be referred to as (junctional) strands in the following description.

The junctions display various geometries which can be classified as follows. *Type 1* (55–60% of the total junctional length) consists of parallel strands with very few or no interconnections (anastomoses) (Fig. 1). *Type 2* junctions (35–40%) have relatively parallel, but often anastomosing strands (Fig. 2). *Type 3* junctions are networks which in many cases appear as a wavy, unstretched variation of Types 1 and 2. Complicated junctions where it is impossible to define an apical-basal "line" across the bundle of junctional strands (i.e., perpendicular to the strands) were excluded from the material used for counting of strands (<5% of the total junctional length). Continuities between the various geometric types of tight junction organization are frequently seen. This junctional architecture may represent "stretch-unstretch transformations" as described by Hull and Staehelin (10). At the basal (abluminal) aspect of the junction, loose loops formed by strands and blind ending strands are often seen. The depth of the junction, excluding loops and blind ending strands, of Types 1 and 2 geometry is in the range of 0.15–0.30 μm.

The mean number of junctional strands in the

TABLE II

Fraction (%; $\bar{x} \pm SD$) of Junction Strands in Complementary Replicas Represented as:

(*a*) Discontinuities in P-face ridges	(*b*) Particles in complementary E-face grooves	(c) Actual discontinuities in the strands (*a* minus *b*)
42.2 ± 4.6	17.8 ± 4.4	24.4 ± 6.5

A total of 27 μm of junctional strands from five different regions (n = 5) with tight junctions were used.

TABLE I

Number of Junction Strands in the Choroid Plexus Epithelium

Rat strain	Lateral ventricle	Third ventricle	Fourth ventricle
Lewis*	7.5 ± 2.6 (n = 229)	7.4 ± 2.2 (n = 124)	7.5 ± 2.4 (n = 383)
Sprague-Dawley‡	7.7 ± 3.4§ (n = 29)	7.4 ± 2.3 (n = 86)	7.3 ± 1.6§ (n = 79)

P + E Fracture Faces; $\bar{x} \pm SD$, n = Number of Measurements.

* Material from 4 rats.

‡ Material from 3 rats.

§ Nonsignificant ($0.4 < p < 0.5$).

choroid plexus epithelium obtained from the lateral, third, and fourth ventricles is shown in Table I. All values (n = 930) are plotted in a histogram

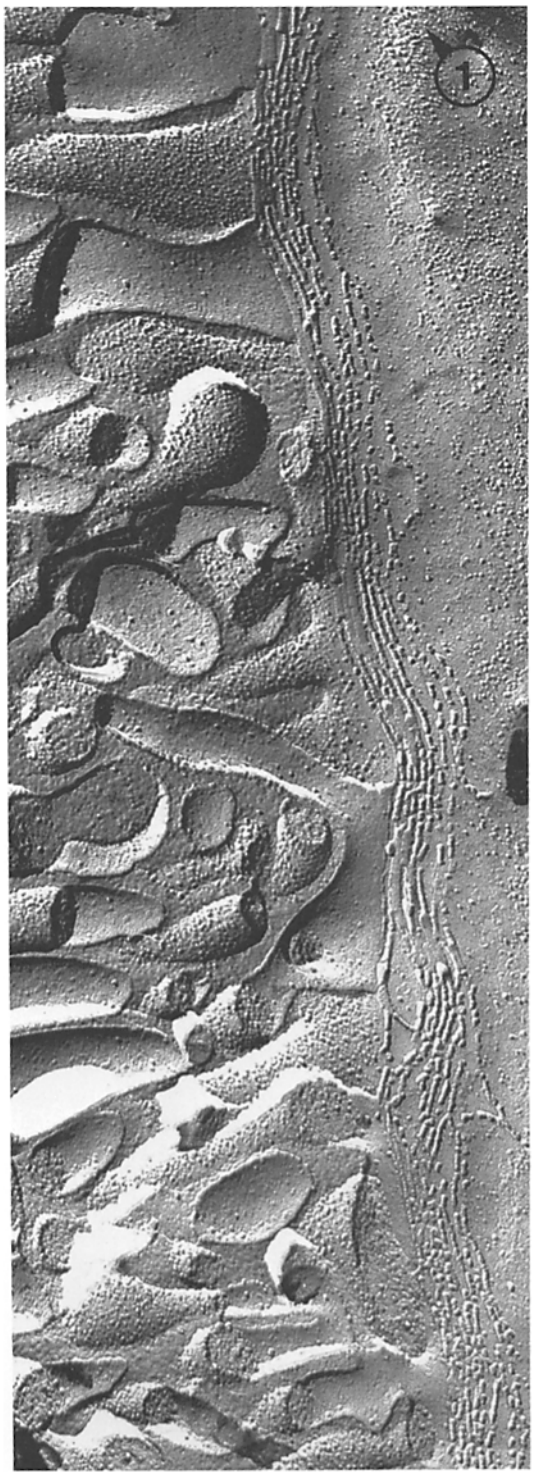

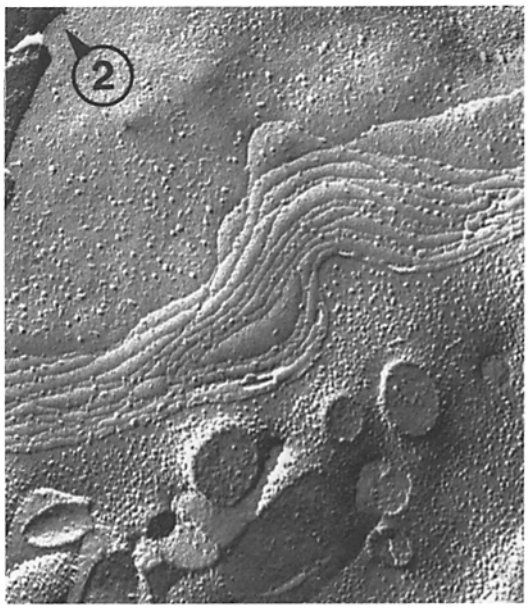

FIGURE 2 Choroid plexus tight junction as it appears on E-faces. Note the numerous, often anastomosing grooves (Type 2 geometry) bearing some scattered particles. × 54,600.

(Fig. 3) which shows that 85.7% of the junctional segments include 5–10 strands. Only 1.1% of the examined junctional segments included as few as 3 strands, and 3.7%, 4 strands. Segments with <3 strands were not seen. At the other end of the spectrum, 8.7% include 11–15, and only 0.9% include >15 strands. Nonsignificant differences in the number of strands in the choroid plexus epithelium from the lateral, third, and fourth ventricles, or between Lewis and Sprague-Dawley rats were seen (Table 1).

No other junctional types (i.e., gap junctions or desmosomes) were observed.

Freeze-Fracture of Unfixed Noncryoprotected Choroid Plexus

Our intention in using this technique was to establish whether the general organization of the

FIGURE 1 Typical arrangement of the choroid plexus epithelial tight junction as it appears on P-faces. The junction is narrow, extending immediately below the apical brush border, and includes 7–8 parallel strands (Type 1 geometry) composed of particles and short bars often with distinct intervening spaces. The arrowhead on the circle surrounding the figure number in this and the following freeze-fracture illustrations indicates the direction of platimum shadowing. × 46,000.

junction was an artifact induced by fixation or cryoprotection. Although considerable technical difficulties exist in freezing fresh choroid plexus tissue directly, the membranes were sometimes rather well preserved, allowing the identification of tight junctions (Fig. 4). In this material no distinct, elongated "bars" were seen. Discontinuous particle chains were present on the E-faces, and delicate grooves containing some particles were sometimes seen on the P-faces (Fig. 4). Useful complementary replicas of unfixed material were not obtained; mismatching of E- and P-faces was very pronounced, probably as a result of plastic deformation, and quantitations of this material could not be performed.

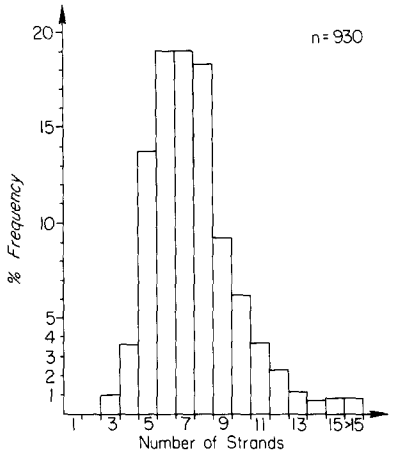

FIGURE 3 Histogram in which the data (n = 930) in Table 1 are represented in graphical form. The spread in the number of junctional strands is clearly seen.

As in glutaraldehyde-fixed tissue, particles were more numerous on the P-faces than on the E-faces of fresh frozen tissue (Fig. 4). Elongated or fibrilar structures occur frequently in the membranes of fresh frozen tissue (Fig. 4). Similar observations have also been reported by Landis and Reese (12) and may be a result of plastic deformation during fracturing of unfixed, and therefore, poorly stabilized intramembrane particles.

Complementary Replicas of Choroid Plexus

When examining regions of routine replicas with transitions between E- and P-faces, it is obvious (and generally assumed in the literature) that the grooves and ridges are "complementary" in their organization. However, to what extent particles on the E-face grooves actually fit into the "discontinuities" in the ridges on the P-face remains uncertain. The complementary replicas of the choroid plexus epithelium show that, although particles in the E-face grooves typically fit well into interspaces of P-face ridges (some minor mismatching can be observed, probably as a result of plastic deformation during the fracturing), "true pores" are present in the junctional strands of the choroid plexus epithelium. The particles present in the grooves in Figs. 5 and 6 do not completely "close" the discontinuities on the corresponding P-face ridges. Another example of apparently true pores in the P-face particle-and-

FIGURE 4 Replica of fresh frozen choroid plexus. The tight junction appears as aligned particles with intervening spaces (small arrows) on the E-face (*E*). On the P-face (*P*), grooves can be seen (large arrows) bearing some particles. More nonjunctional particles are seen on the P-face than on the E-face. Note the fibrous intramembrane structures (asterisk) characteristic of unfixed and noncryoprotected tissue. × 82,300.

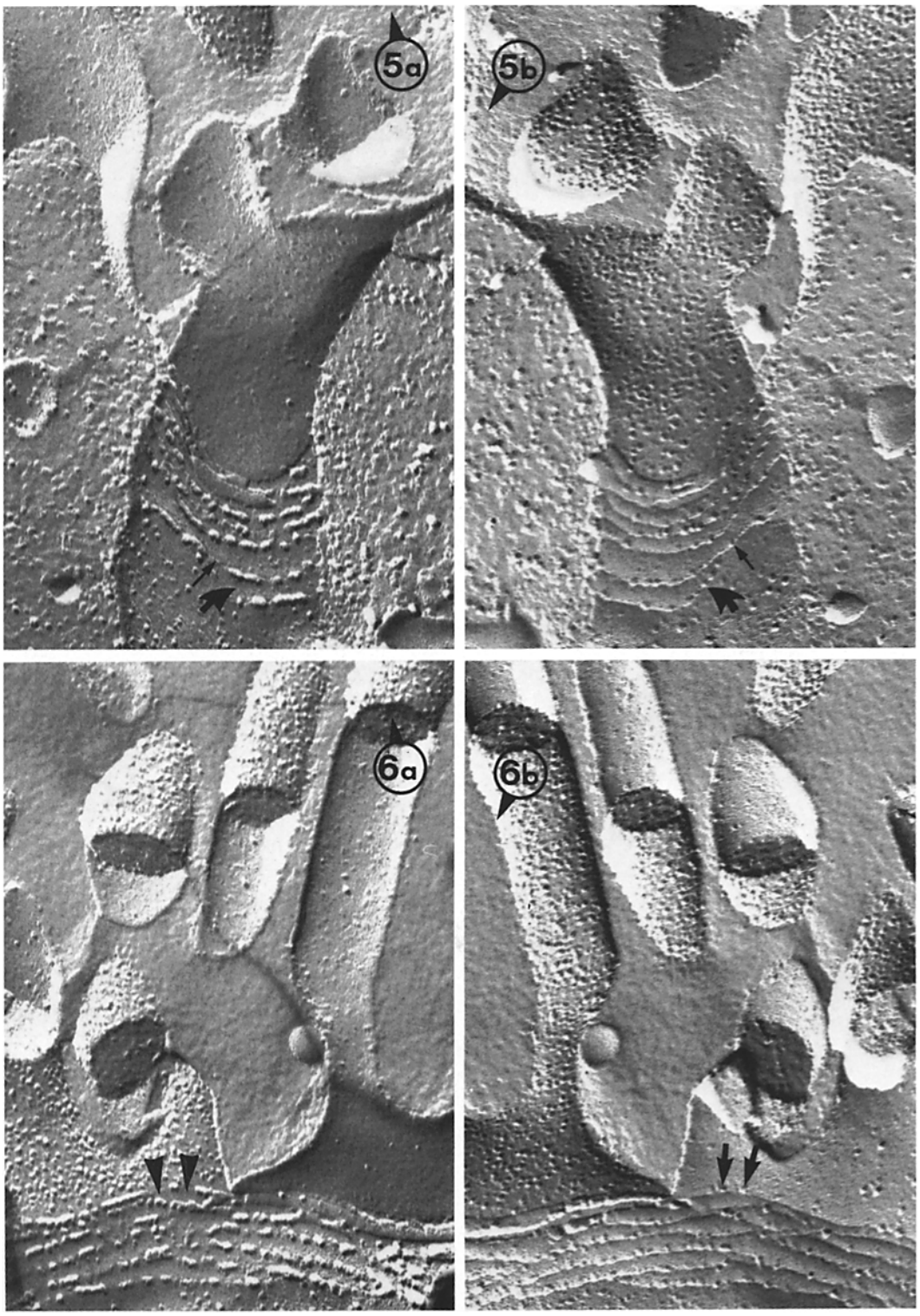

FIGURE 5 (*a* and *b*) Complementary replicas of choroid plexus showing P-face (*a*) and E-face (*b*) of a tight junction. While the most basal strand in *a* apparently ends blindly, a distinct groove with some particles is seen in *b* (curved arrows). The small arrows indicate a gap in a P-face ridge (*a*) which cannot be completely "closed" by the corresponding particle in the E-face groove (*b*). × 97,000.

FIGURE 6 (*a* and *b*) In these complementary replicas of the choroid plexus, two gaps in the P-face ridges are indicated (*a*, arrowheads) which cannot be completely plugged by the corresponding particles (*b*, arrows) in the E-face grooves. × 90,200.

bar chains is seen in Fig. 7. Here, there are obviously fewer particles in the E-face grooves than discontinuities in the corresponding P-face ridges.

The fraction of the junctional strands represented as P-face discontinuities, E-face particles, and actual discontinuities in the strands is shown in Table II. The mean width of the discontinuities (P-face discontinuities minus corresponding E-face groove particles) is 7.7 ± 4.5 nm (n = 66). Fig. 10 is a histogram of the frequencies of widths.

Although more or less densely packed particle clusters sometimes occur within the junction, and especially between blind ending strands (Fig. 8), these clusters were never associated with complementary regions of E-face pits in double replicas, and therefore, could not be classified as gap junctions (see also reference 27). The complementary replicas show a general good matching of corresponding nonjunctional areas from the two replicas. However, the distribution of nonjunctional particles on the P-face is not uniform, as patches without particles occur. In some cases, the use of complementary replicas established that the corresponding area on the E-face is also devoid of particles (Fig. 9) in contrast to what might be expected.

Complementary Replicas of Small Intestine

In intestinal tissue fixed conventionally in 2.5% glutaraldehyde, the tight junctions of the epithelium appeared as rather continuous ridges on the P-faces, and as almost particle-free, continuous grooves on the E-faces (Fig. 11), thus being in contrast to the architecture of the choroid plexus epithelial junctions. Furthermore, complementary replicas showed a good matching of the particles in the E-face grooves and the discontinuities in the P-face ridges (Fig. 11). ~5% of the tight junctional strands in the intestinal material was found to be discontinuous.

As mentioned above for the choroid plexus, complementary replicas of unfixed tissue were of a very poor quality (see also reference 5). We therefore used a brief fixation in very dilute glutaraldehyde. Complementary replicas of this material supported the view that a reasonable matching of E- and P-faces is impossible to obtain in poorly fixed or unfixed material. For example, particle chains rather than a particle-free groove sometimes corresponded to a fibril (Fig. 12).

DISCUSSION

Technical Considerations

The present study reports an analysis of tight junctions by means of freeze-fracture. Data obtained in this way should be evaluated with care, and, as emphasized by Wade et al. (30), the analysis of complementary replicas and of fresh frozen tissue is very important in our efforts to correlate structural observations with physiological data. The use of these two techniques, however, focuses at certain problems with respect to particle loss and plastic deformation during fracturing.

By using fresh frozen tissue, we could establish that, in the case of the choroid plexus epithelium, glutaraldehyde fixation and glycerol cryoprotection do not cause significant alterations in the general architecture of the tight junction. Thus, particles rather than continuous fibrils are the main component of the junctional strands. The tendency to form short bars after glutaraldehyde fixation may be a result of the cross-linking effect of the fixative (van Deurs and Luft, in preparation). Similar observations have been reported for the junctions of the small intestine (23). The significance of the observation that in unfixed material the junctional particles are present on the E-face rather than on the P-face is uncertain (and is under further investigation) but should not interfere with the present study which deals with the "total amount" of junctional material. Unfortunately, obtaining "good" complementary replicas of fresh frozen tissue (or tissue fixed briefly in dilute glutaraldehyde), especially for quantitative analysis, seems at present to be an overwhelming technical problem. This may not be true for isolated cells or cell fragments. However, the correspondence in the junctional architecture between fixed and unfixed choroid plexus, and the difference in junctional architecture between choroid plexus and small intestine, makes it unlikely that the particulate nature of tight junctional strands of the choroid plexus epithelium would be "artificial," e.g., because of deformation of continuous fibrils.

Other factors (4) to be considered in the evaluation of the present freeze-fracture data are: (*a*) the influence of the platinum thickness and the shadowing angle on the quantitative measurements (the pores "in vivo" are probably wider than calculated here); (*b*) contamination, which

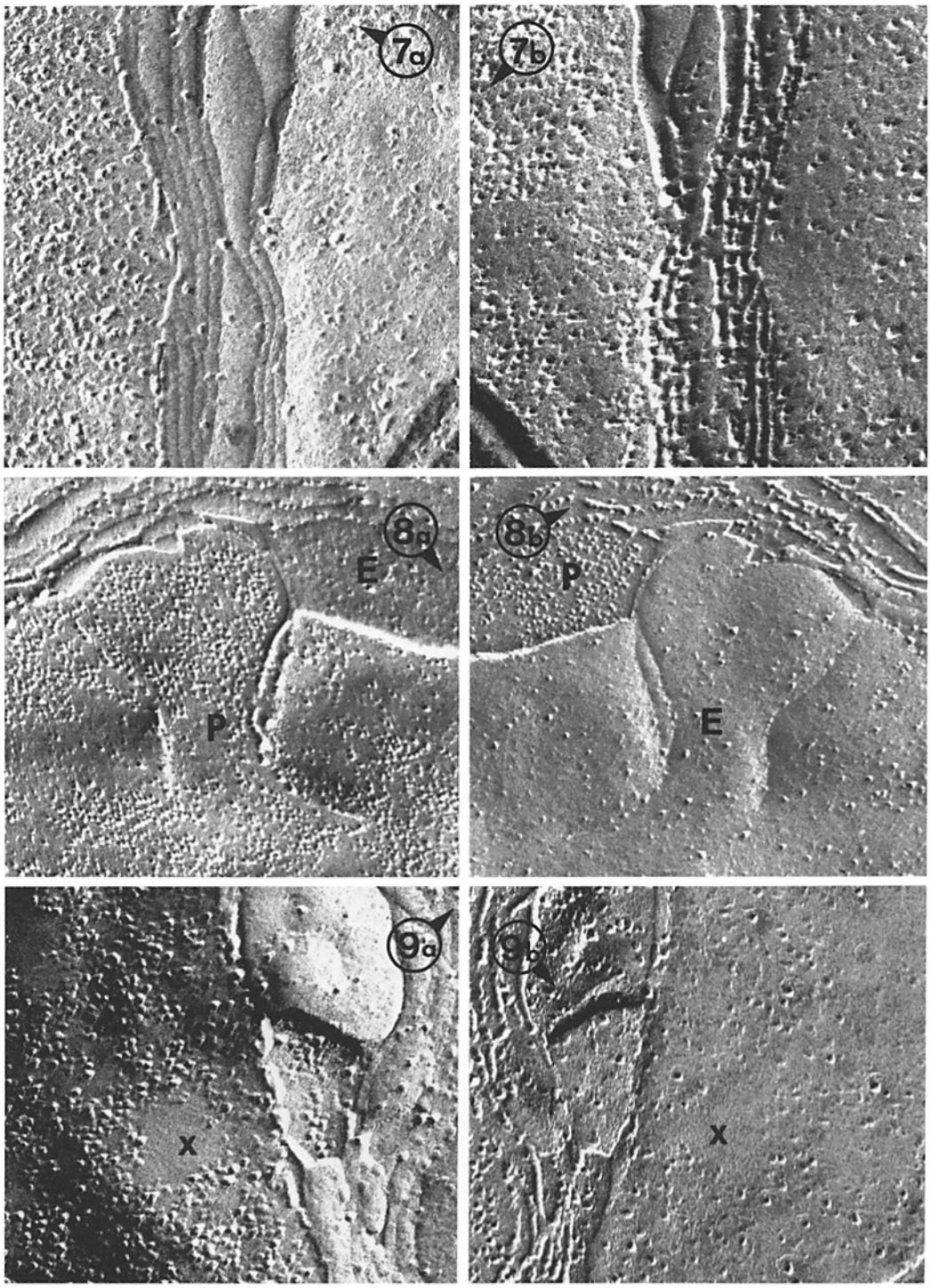

FIGURE 7 (*a* and *b*) Complementary replicas of a tight junction from the choroid plexus. Note that there are more discontinuities in the P-face ridges (*b*) than particles in the E-face grooves (*a*). × 105,000.

FIGURE 8 (*a* and *b*) Complementary replicas of a tight junction and associated intramembrane areas abluminal to the junction. Note the complementary P- and E-face (*P* and *E*) areas between the blind ending strands. × 79,000.

FIGURE 9 (*a* and *b*) Complementary replicas showing a nonrandom distribution of intramembrane particles: the area marked X is particle free in both the P-face (*a*) and E-face (*b*). × 105,000.

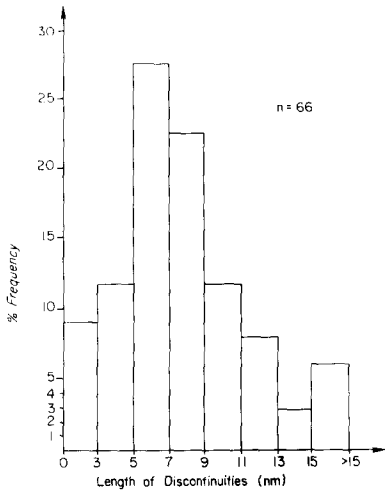

FIGURE 10 Histogram showing the frequencies of the widths (lengths) of discontinuities in the junctional strands of the choroid plexus epithelium (width of discontinuities in P-face ridges minus particles in complementary E-face grooves).

can be minimized by proper operation of the Balzers apparatus; (*c*) plastic deformation, which may cause dislocation and distortion of particles from the P-face ridges and E-face grooves, or conceivably a particle could be pulled into two parts, seen opposite each other and thus "measured" twice. Plastic deformation seems to be especially pronounced in poorly fixed or unfixed tissue. To what extent plastic deformation influences the quantitative data obtained by matching complementary replicas cannot be estimated in the present study. Additionally: (*d*) some particles may simply become lost during the fracturing process. While it is reasonable to expect the presence of continuous grooves complementary to junctional fibrils (e.g., in the small intestine), it is difficult to explain how the discontinuous particle chains of the choroid plexus epithelial junctions also exhibit complementary, continuous grooves. This may indicate that junctional material actually is lost during fracturing. However, in a study of tight junction development in the fetal liver, Montesano et al. (16) found that in the early stages of development, where the junctional strands appear as rows of particles, the presumptive complementary E-face structure was also continuous grooves rather than rows of pits. Furthermore, the present "control" experiments with small intestine revealed a good matching between the few discontinuities in the P-face ridges and particles in the E-face grooves. This observation does not make it likely that particles should be lost to any significant degree during fracturing. The question of whether particles are lost during fracturing is thus difficult to elucidate at present, but may represent a serious source of error in freeze-fracture studies in general.

Interpretation of Results

A correlation between transepithelial permeability (maintenance of ionic and osmotic gradients) and the number of tight junctional strands in some epithelia has been established by Claude and Goodenough (7). Thus, in "leaky" epithelia the number of strands is low (mean value 1–4, range 1–6), while in "tight" epithelia the number of strands is high (mean value 5–10, range 4–14). Electrophysiological studies on the choroid plexus of the frog (33, 34) and cat (32) revealed a relatively high conductance in this epithelium, 5.4 m-mho/cm^2 and 6.3 m-mho/cm^2, respectively. We, therefore, expected that the mean number of junctional strands in the "leaky" choroid plexus epithelium would be <5, but found instead a mean value of ~ 7.5, independent of the rat strain and the ventricle from which the plexus was obtained. According to the criteria of Claude and Goodenough (7), a mean of 7.5 strands indicates a "tight" or "very tight" epithelium. However, lack of correlation between the number of tight junctional strands and transepithelial permeability has previously been reported (14, 15, 19). Martinez-Palomo and Erlij (14) suggested that parameters in addition to number of strands, i.e., features of the strands themselves, may be of importance with respect to permeability properties. The present results obtained by examination of complementary replicas and comparison of choroid plexus epithelium and small intestinal epithelium suggest that the numerous strands of the "leaky" tight junction in the choroid plexus epithelium may be provided with "pores" which may represent hydrated channels allowing penetration of ions, as suggested on physiological grounds by Wright (33), and on morphological grounds (by examination of routine replicas) by Brightman et al. (1, 2).

A general problem in the freeze-fracture analysis of tight junctions in relation to paracellular permeability properties is that the fracture reveals structures within the membrane, and not between the membranes. If the tight junction is represented by one "fibril" between the two adjacent

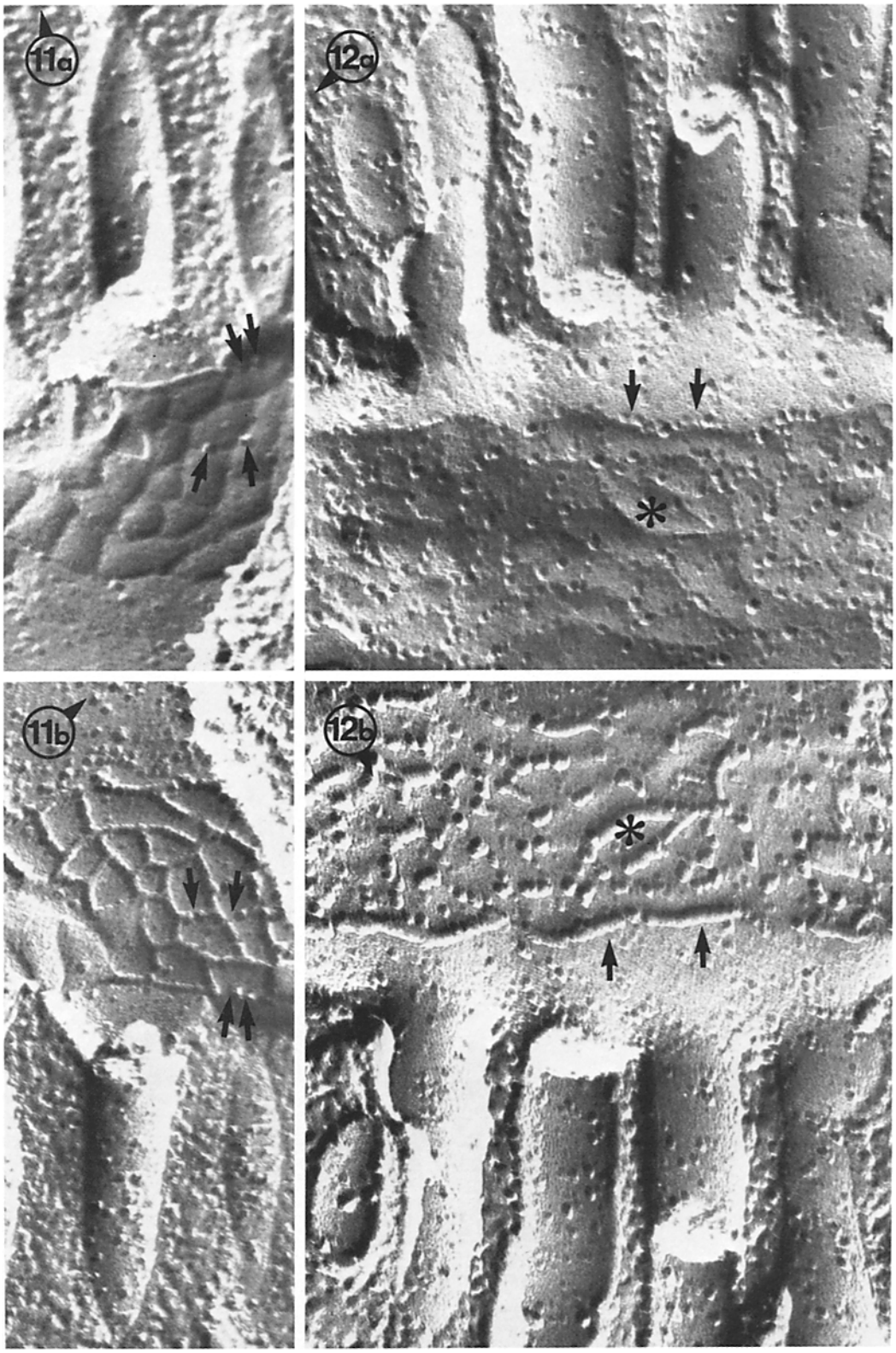

FIGURE 11 (*a* and *b*) Complementary replicas of a tight junction in the small intestine epithelium. Arrows indicate discontinuities in the P-face ridges (*b*) and corresponding particles in the E-face furrows (*a*). The matching is good, and the junctional strands are almost continuous. × 150,000.

FIGURE 12 (*a* and *b*) Complementary replicas of poorly fixed small intestine. Matching between the P-face ridges (*b*) and the E-face grooves (*a*) is far from perfect. While the asterisk indicating a particle-free groove and a complementary fibril, the arrows show a particle chain complementary to a fibril. × 150,000.

membranes (29), discontinuities in the fibrils seen on the fracture faces can readily be interpreted as discontinuities in the paracellular diffusion barrier. If, on the other hand, the "two-fibril model" (6) is considered, a discontinuity in the fibrils seen on the fracture faces may not necessarily influence the permeability of the paracellular pathway. Which model to prefer is, however, still a matter of controversy (5).

The CSF of early fetuses contains higher concentrations of ions, nonelectrolytes, and protein than in later stages. Møllgaard et al. (19) reported that the tight junctional architecture of the choroid plexus epithelium did not change during fetal (sheep) development and they found a mean number of junctional strands of ~3.5 both in earlier and later stages. They suggested that tight junctions were already well developed in early stages and therefore proposed an alternative explanation for the apparently high leakiness of the early plexus: a transport system across the epithelial cells formed by endoplasmic reticulum connecting both the luminal and abluminal surfaces (19, 20). However, such a transcellular tubular system cannot be established in the epithelium of the adult rat choroid plexus (24, 25, 28), and pores in the junctional strands therefore seem to be a likely explanation of the relatively high leakiness in the adult choroid plexus epithelium.

To what extent apparent discontinuities in tight junction P-face ridges may actually represent true pores in tissue other than the choroid plexus is at present uncertain. However, as shown in the present study, "tighter" tight junctions characteristically (under normal physiological conditions) exhibit only few discontinuities (see also reference 7), and consequently, only a few pores, even if P-face discontinuities do not have matching particles in E-face grooves. Schneeberger et al. (22) investigated the tight junctions of various stages of fetal lung development in lambs. Along with the development and increasing tightness of the junctions, an increase in number of strands occurred, as well as a change from particulate to more continuous strands. Furthermore, complementary replicas of the later stages showed that P-face discontinuities were not a result of absence of particles, in contrast to what we suggest here for the leaky choroid plexus tight junction. In the latest stages of lamb lung development the P-face ridges were continuous, and the E-face grooves were particle free. Support for discontinuities being responsible for high permeability properties also comes from experiments with toad stomach epithelium. Brightman et al. (1) found that exposure of this epithelium to hyperosmotic urea caused more discontinuities in the junctional strands, an observation they related to increased permeability. A change in liver tight junctions from fibrillar to particulate has also been reported after treatment with hypertonic disaccharides (9). Furthermore, Humbert et al. (11) showed that, in the proximal tubules of *Necturus* undergoing saline diuresis, a situation which makes the tight junction more leaky, the number and length of discontinuities in the junctional strands increase.

In conclusion, we have shown that the problem of explaining the relatively high permeability characteristics in an epithelium having a rather large number of tight junctional strands may be attacked by a detailed examination of complementary replicas. The results of such an analysis can be interpreted as indicating the presence of definite discontinuities or pores in the tight junctional strands, although the importance of particle loss during fracturing remains as a possible artifact needing more attention and investigation in the future.

The authors express thanks to Dr. Robert Bolender for critically reading the initial version of the manuscript and providing valuable suggestions. Mr. Eng Chuan Teh lent technical assistance in some phases of this work and Ms. Doris Ringer provided secretarial help with the manuscript.

Portions of this research were supported by U. S. Public Health Service grant RR-05432 from the National Institutes of Health.

Received for publication 21 April 1978, and in revised form 27 October 1978.

REFERENCES

1. Brightman, M. W., L. Prescott, and T. S. Reese. 1975. Intercellular junctions of special ependyma. *In* Brain-Endocrine Interaction II. The Ventricular System. K. M. Knigge, D. E. Scott, H. Kobayashi, and S. Ishii, editors. 2nd Int. Symp. Shizuoka. 1974. Karger, Basel. 146–165.
2. Brightman, M. W., R. R. Shivers, and L. Prescott. 1975. Morphology of the walls around fluid compartments in nervous tissue. *In* Fluid Environment of the Brain. H. F. Cserr, J. D. Fenstermacher, and V. Fencl, editors. Academic Press, Inc., New York. 3–24.
3. Bullivant, S. 1974. Freeze-etching techniques applied to biological membranes. *Philos. Trans. R. Soc. Lond. B. Biol. Sci.* **268**:5–14.
4. Bullivant, S. 1977. Evaluation of membrane structure facts and artefacts produced during freeze-fracturing. *J. Microsc. (Oxf.).* **111**: 107–116.
5. Bullivant, S. 1978. The structure of tight junctions. *In* Electron Microscopy III. J. M. Sturgess, editor. Ninth International Congress on Electron Microscopy, Toronto. 659–672.
6. Chalcroft, J. P., and S. Bullivant. 1970. An interpretation of liver cell membrane and junction structure based on observation of freeze-fracture replicas of both sides of the fracture. *J. Cell Biol.* **47**:49–60.
7. Claude, P., and D. A. Goodenough. 1973. Fracture faces of zonulae

occludentes from "tight" and "leaky" epithelia. *J. Cell Biol.* **58:**390–400.

8. DAVSON, H. 1972. The blood-brain barrier. *In* The Structure and Function of Nervous Tissue, Vol. IV. G. H. Bourne, editor. Academic Press, Inc., New York. 321–445.
9. GOODENOUGH, D. A., and N. B. GILULA. 1974. The splitting of hepatocyte gap junctions and zonulae occludentes with hypertonic desaccharides. *J. Cell Biol.* **61:**575–590.
10. HULL, B. E., and L. A. STAEHELIN. 1976. Functional significance of the variations in the geometrical organization of tight junction networks. *J. Cell Biol.* **68:**688–704.
11. HUMBERT, F., A. GRANDCHAMP, C. PRICAM, A. PERRELET, and L. ORCI. 1975. Morphological changes in tight junctions of *Necturus maculosus* proximal tubules undergoing saline diuresis. *J. Cell Biol.* **69:** 90–96.
12. LANDIS, D. M. D., and T. S. REESE. 1975. Membrane structure in rapidly frozen, freeze-fractured cerebellar cortex. *J. Cell Biol.* **63**(2, Pt. 2):184*a*. (Abstr.).
13. MACKENZIE, A. P. 1969. Apparatus for the partial freezing of liquid nitrogen for the rapid cooling of cells and tissues. *Biodynamica.* **10:** 341–351.
14. MARTÍNEZ-PALOMO, A., and D. ERLIJ. 1975. Structure of tight junctions in epithelia with different permeability. *Proc. Natl. Acad. Sci. U. S. A.* **72:**4487–4491.
15. MAZURKIEWICZ, J. E., J. S. ADDIS, and R. J. BARRNETT. 1977. Tight junctions of the secretory epithelium of the avian salt gland: a freeze fracture study. *J. Cell Biol.* **75**(2, Pt. 2):71*a*. (Abstr.).
16. MONTESANO, R., D. S. FRIEND, A. PERRELET, and L. ORCI. 1975. In vivo assembly of tight junctions in fetal rat liver. *J. Cell Biol.* **67:**310–319.
17. MOOR, H. 1971. Recent progress in the freeze-etching technique. *Philos. Trans. R. Soc. Lond. B. Biol. Sci.* **261:**121–131.
18. MÜHLETHALER, K., W. HAUENSTEIN, and H. MOOR. 1973. Double fracturing method for freeze-etching. *In* Freeze-Etching. Techniques and Applications. E. L. Benedetti and P. Favard, editors. Société Francaise de Microscopie Electronique, Paris. 101–106.
19. MØLLGÅRD, K., D. H. MALINOWSKA, and N. R. SAUNDERS. 1976. Lack of correlation between tight junction morphology and permeability properties in developing choroid plexus. *Nature (Lond.).* **264:**293–294.
20. MØLLGÅRD, K., and N. R. SAUNDERS. 1977. A possible transepithelial pathway via endoplasmic reticulum in foetal sheep choroid plexus. *Proc. R. Soc. Lond. B. Biol. Sci.* **199:**321–326.
21. QUINTON, P. M., E. M. WRIGHT, and J. McD. TORMEY. 1973. Localization of sodium pumps in the choroid plexus epithelium. *J. Cell Biol.* **58:**724–730.
22. SCHNEEBERGER, E. E., D. V. WALTERS, and R. E. OLVER. 1978. Development of intercellular junctions in the pulmonary epithelium of the foetal lamb. *J. Cell Sci.* **32:**307–324.
23. STAEHELIN, L. A. 1973. Further observations on the fine structure of freeze-cleaved tight junctions. *J. Cell Sci.* **13:**763–786.
24. VAN DEURS, B. 1978. Horseradish peroxidase uptake into the rat choroid plexus epithelium, with special reference to the lysosomal system. *J. Ultrastruct. Res.* **62:**155–167.
25. VAN DEURS, B. 1978. Microperoxidase uptake into the rat choroid plexus epithelium. *J. Ultrastruct. Res.* **62:**168–180.
26. VAN DEURS, B. 1978. Cell junctions in the choroid plexus epithelium. *Anat. Rec.* **190:**569–570. (Abstr.).
27. VAN DEURS, B., and J. K. KOEHLER. 1978. Organization of tight junctions in the choroid plexus epithelium. *In* Electron Microscopy II. J. M. Sturgess, editor. Ninth International Congress on Electron Microscopy, Toronto. 336–337.
28. VAN DEURS, B., M. MØLLER, and O. AMTORP. 1978. Uptake of horseradish peroxidase from CSF into the choroid plexus of the rat, with special reference to transepithelial transport. *Cell Tissue Res.* **187:** 215–234.
29. WADE, J. B., and M. J. KARNOVSKY. 1974. The structure of the zonula occludens. A single fibril model based on freeze-fracture. *J. Cell Biol.* **60:**168–180.
30. WADE, J. B., W. A. KACHADORIAN, and V. A. DISCALA. 1977. Freeze-fracture electron microscopy: relationship of membrane structural features to transport physiology. *Am. J. Physiol.* **232:**F77–F83.
31. WEHRLI, E., K. MÜHLETHALER, and H. MOOR. 1970. Membrane structure as seen with a double replica method for freeze fracturing. *Exp. Cell Res.* **59:**336–339.
32. WELCH, K., and H. ARAKI. 1975. Features of the choroid plexus of the cat, studied *in vitro*. *In* Fluid Environment of the Brain. H. F. Cserr, J. D. Fenstermacher, and V. Fencl, editors. Academic Press, Inc., New York. 157–165.
33. WRIGHT, E. M. 1972. Mechanisms of ion transport across the choroid plexus. *J. Physiol.* **226:**545–571.
34. WRIGHT, E. M. 1975. Solute transport across the frog choroid plexus. *In* Fluid Environment of the Brain. H. F. Cserr, J. D. Fenstermacher, and V. Fencl, editors. Academic Press, Inc., New York. 139–156.